Dual color x rays from Thomson or Compton sources

V. Petrillo,[1,2] A. Bacci,[1] C. Curatolo,[1,2] M. Ferrario,[3] G. Gatti,[3] C. Maroli,[2] J. V. Rau,[4] C. Ronsivalle,[5] L. Serafini,[1] C. Vaccarezza,[3] and M. Venturelli[2]

[1]*INFN Milano, Via Celoria, 16 20133 Milano, Italy*
[2]*Università degli Studi di Milano, Via Celoria, 16 20133 Milano, Italy*
[3]*LNF, INFN Via E. Fermi, 40 Frascati (Roma), Italy*
[4]*ISM-CNR Via del Fosso del Cavaliere, 100 00133 Roma, Italy*
[5]*ENEA Via E. Fermi, 45 Frascati (Roma), Italy*

(Received 12 September 2013; published 28 February 2014)

We analyze the possibility of producing two-color x or γ radiation by Thomson/Compton backscattering between a high intensity laser pulse and a two-energy level electron beam, constituted by a couple of beamlets separated in time and/or energy obtained by a photoinjector with comb laser techniques and linac velocity bunching. The parameters of the Thomson source at SPARC_LAB have been simulated, proposing a set of realistic experiments.

DOI: 10.1103/PhysRevSTAB.17.020706 PACS numbers: 41.20.Jb

I. INTRODUCTION

The development of x-ray sources characterized by high versatility, large spectral flux and tunability opens the way for a real breakthrough in a wide number of scientific and technical fields. One of the most promising formats in which the x radiation can be delivered to the users is in the form of packets containing two different spectral lines with adjustable time separation between them. By means of two color x rays it is possible to deepen the fundamental knowledge and understanding of the properties of materials and living systems, probing the matter on atomic scale in space and time [1]. Pairs of colored x-ray pulses can be particularly useful to perform pump and probe experiments of structural dynamics, a very important class of experiments designed to monitor the ultrafast changes in atomic, electronic and magnetic structure [2–4]. In the pump-probe experiments the process—e.g., a chemical reaction or an excitation or a structural change in a solid state—is started with one first pulse and then, after a certain time, a second one of another color is used to get the image of the event. In this way, following its time evolution, information on pathways, barriers and transition states of the process can be gained. This could even extend the knowledge further with respect to the Nobel Prize work on femtochemistry of Zewail [5]. The time-domain spectroscopy is indeed based on the interplay between the conjugate variables of frequency and time [6,7]. The time scale for such dynamics can range from 10 fs in ultrafast processes as the dissociative ionization [8], to hundred femtoseconds for less energetic chemical mechanisms [9,10]. Another important issue is the future color x-ray technology. Color x-ray imaging is a technique that will provide significant development to screening or diagnostic mammography. The color component contains extra information and allows one to discriminate the chemical composition of the absorbing tissues [11,12].

Experiments of dual color production and use have been recently carried on with free-electron lasers (FELs) as radiation sources [4,13–17] and several promising proposals aimed to generate two-color FEL emission in the x-ray wavelength regime [18–21] have been so far investigated.

Thomson and Compton sources, even though less brilliant with respect to FELs, produce radiation with short wavelength, high power, ultrashort time duration, large transverse coherence and tunability, ensuring, at the same time, contained dimensions of the setup and limited costs of construction and maintenance. Existing Thomson sources [22–32] have already demonstrated to be an important tool for generating tunable quasimonochromatic x/γ rays suitable for applications in many fields such as crystallography, plasma, high energy, matter physics and nuclear photonics and in the advanced biomedical imaging. In fact, experiments on phase contrast imaging [25,27], microtomography [25], K-edge techniques [23,33] on biological and human samples have been successfully performed.

The Thomson source SL_Thomson [34] at SPARC_LAB [35] is operating at INFN-LNF and foresees high flux and large versatility. It is based on the backscattering between the light pulse provided by the high intensity Ti:sapphire laser FLAME [36] and the high brightness electron beam of the photoinjector SPARC [37]. SPARC delivers electron bunches with charge up to 1 nC, energy up to 170 MeV, and brightness larger than 10^{14} A/mrad^2. Since the first application of SL_Thomson is in the field of mammographic images, the photoinjector

is foreseen to operate, in a first stage, at a final electron energy E_e of about 30 MeV, producing Doppler blueshifted hard x rays with energy $E_p = 4E_0\gamma^2$ ($E_0 = 1.55$ eV is the photon energy of FLAME and the Lorentz factor $\gamma \approx 60$) of about 20 keV. The SPARC standard operation at 150 MeV permits one to approach values of $E_p \approx 500$ keV, spanning the range within these limits, and, with a future upgrade that will bring the electrons to 250 MeV, γ rays with energies exceeding 1 MeV could be produced.

At SPARC_LAB, electron beams bichromatic in energy have been produced by using the technique of illuminating the photocathode with a comb laser pulse and by rotating the electron phase space during the acceleration by means of the velocity bunching in the linac. In this way, the time distance between the two beamlets and their energies can be controlled in dependence of the injection phases. Such e-bunches have been matched to and transported into the undulator with FEL emission of double color radiation at a wavelength of 800 nm [16].

In this paper, we describe the possibility of obtaining two-color x rays with the Thomson/Compton backscattering between a laser pulse and the same aforementioned two-energy level electron beams that were produced and tested during the dual color FEL operations. Other possible methods of obtaining two-color Thomson radiation, not available so far at SPARC, rely on the use of two lasers with different frequency or on the interaction at two different angles and will be studied in the future. The use of two-color electron beams, instead, can already be implemented at SPARC and is part of the plans for the near future. In the first section we will describe the electron beam production and simulation in cases with different energy and temporal separations. The second section will be devoted to the study of the radiation characteristics, proposing possible experiments at SPARC. Then, we will close with comments and conclusions.

II. TWO-ENERGY LEVEL ELECTRON BEAMS

Electron beams with a double energy level structure have been routinely produced and extensively studied at SPARC_LAB [38,39] with several different applications. The procedure consists in the generation of a comb laser radiation produced by passing the cathode laser through a birefringent β-barium borate crystal, thus obtaining two pulses long hundreds fs, spaced by few ps. The distance between the two laser pulses is controlled by changing the crystal length. The photoemitted, ps-spaced, electron beam is injected into the first accelerating structure close to the zero crossing radio frequency (rf) field phase and then propagated along the linac. Since, during the earlier stage, the beam velocity is much lower than the phase velocity of the rf wave, the electrons slip back to phases where the field is accelerating, being chirped and compressed at the same time. The method has been applied not only for producing one short electron bunch [40,41], but also for the controlled compression of sequences of pulses with application in the FEL and terahertz fields [42]. Two-energy level electron beams, similar to those used in the FEL two-color experiments [16], have been simulated with beam dynamical codes as Tstep [43] and Astra [44]. The linac SPARC is constituted by three S-band accelerating cavities SLAC type, the first two embedded by magnetic solenoids for the emittance control. In the first example (Table I, column A), the linac rf phases are set in such a way to extract the beam before the condition of maximum compression, when the rotation of the bunch in the phase space, responsible for the separation in energy and time of the two beamlets, is not completed. The longitudinal phase space of the electrons at the end of the linac, Fig. 1, panel (1), shows that the two beamlets, named (a) and (b), are split both in time and in energy. The partial current profiles of both bunches are shown together with the total one in panel (2), while the energy distributions are in panel (3). The beamlets are overlapping in time only in the central part. The whole beam has a peak current of about 110 A, with 630 fs rms pulse duration at energies of about 80 MeV. The energy difference δE_e between the beamlets is about 1 MeV. The second example, presented in Fig. 2, concerns a case where the electron beam (Table I, column B) is extracted closer to the maximum compression condition, the two beamlets overlap better and are separated by an energy gap of about $\delta E_e = 1.4$ MeV. As regards the transverse distribution, beam (A) presents two beamlets well balanced, with same radii and similar momentum distribution. In the case of

TABLE I. Main parameters of electron, laser, and radiation beams.

	Beam (A) Beamlet 1	Beam (A) Beamlet 2	Beam (A)	Beam (B) Beamlet 1	Beam (B) Beamlet 2	Beam (B)
Charge Q (pC)	125	125	250	125	125	250
Energy E (MeV)	79.46	80.48	80	79.3	80.7	80
Energy spread (MeV)	0.61	0.59	0.6	0.66	0.54	0.6
Horizontal emittance (mm mrad)	1.87	1.87	1.87	1.1	0.75	0.9
Vertical emittance (mm mrad)	1.86	1.86	1.86	1.05	0.74	0.9
Laser waist (m)	25			25		
Mean photon energy (keV)	148			148		

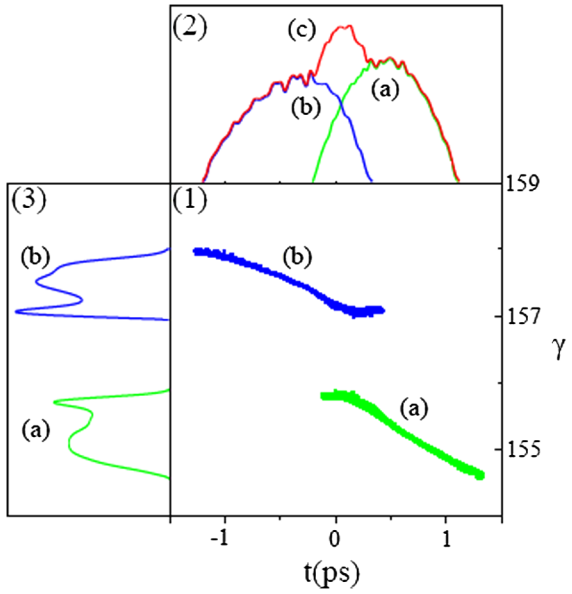

FIG. 1. Beam A—Simulation by TSTEP. (1) Phase space. (a) Low energy and (b) high energy beamlets. (2) Total (c) and partial [(a) and (b)] electron current. (3) Energy distribution.

beam (B), instead, even if it is better as regards the global parameters, the two beamlets have different radii and different emittance, the lower energy one being worse than the other one. These beams are the simulations of two different working points used in the two-color FEL experiment and discussed in [16].

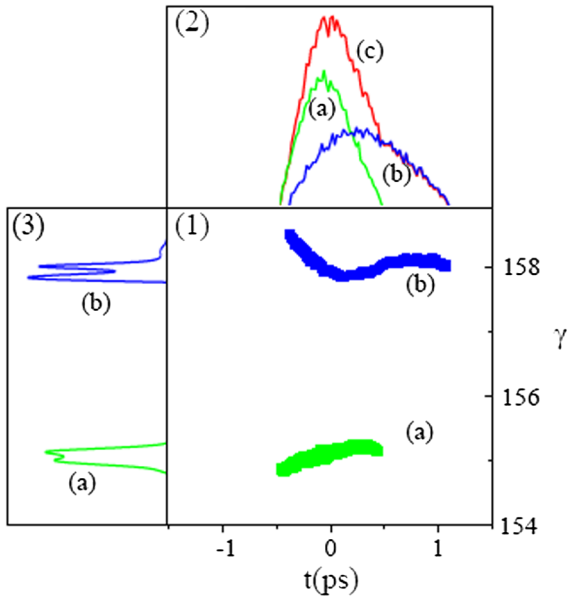

FIG. 2. Beam B—Simulation by ASTRA. (1) Phase space. (a) Low energy and (b) high energy beamlets. (2) Total (c) and partial [(a) and (b)] electron current. (3) Energy distribution.

III. RADIATION CHARACTERISTICS

At the exit of the linac, the electron beam is focused by a system set before the interaction chamber, where it meets the electromagnetic field of the laser pulse, and is constituted by three magnetic quadrupoles and a solenoid. The geometry of the scattering is described in Fig. 3. The electron beam propagating along the z direction impinges the laser radiation at an angle α close to 180°.

Each electron, characterized by normalized velocity $\underline{\beta}_i$ forming an angle θ_i with the z axis, scatters photons with frequency ν_p given by

$$\nu_p = \nu_0 \frac{1 - \underline{e}_k \cdot \underline{\beta}_i}{1 - \underline{n} \cdot \underline{\beta}_i + \frac{h\nu_0}{mc^2\gamma_i}(1 - \underline{e}_k \cdot \underline{n})}, \tag{1}$$

where ν_0 is the frequency of the incident laser photon, $\underline{e}_k$ the unit vector of its direction, $\underline{n}$ is the direction of the scattered photon, h the Planck constant and γ_i the electron Lorentz factor before the scattering. The last term in the denominator is related to the quantum red shift, and is important only when the Lorentz factor of the electron beam approaches the GeV [45]. The classical model describing the interaction between electron and radiation, based on the fundamental laws of the electromagnetism [46], has been widely analyzed in the framework of the development of Thomson sources and cross-checked versus experiments. The well-known result is that, in the far zone, the spectral-angular distribution of the photons emitted by the ith electron is given by the relation involving the Fourier transform of the retarded current:

$$\frac{dN_i}{d\nu_p d\Omega} = \alpha\nu_p \left| \int dt \underline{n} \times \underline{n} \times \underline{\beta}_i(t) e^{i\omega[t - \underline{n}\cdot\underline{r}_i(t)/c]} \right|^2, \tag{2}$$

where $\underline{r}_i(t)$ is the position of the electron, $\alpha = 1/137$ is the fine structure constant and cgs units are used throughout. Considering negligible the correlations between the electrons that could give rise to collective effects [47,48], and in a linear or moderately nonlinear regime [49,50], the

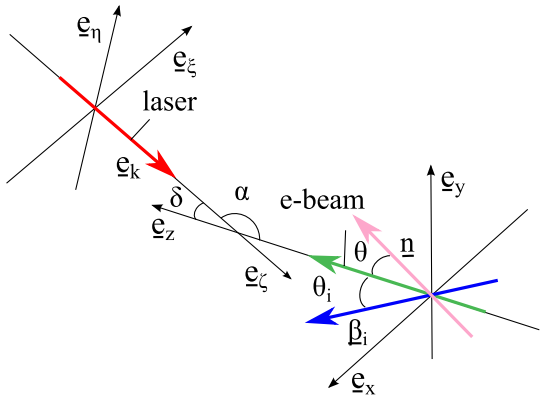

FIG. 3. Geometry of the interaction.

generalization to an ensemble of electrons can be made by summing over the whole beam the contributions of the single particles. As regards the interacting field, Gaussian functions describe correctly the profiles, with the normalized electric field A_L given by the expression

$$A_L = \frac{E_L e^{-\frac{\xi^2+\eta^2}{2\sigma_T^2(1+\frac{\zeta^2}{Z_R^2})} - \frac{(\zeta - ct\cos\alpha)^2}{2\sigma_z^2} + i\varphi}}{h\nu_0(2\pi)^{3/2}\sigma_T^2\sigma_z\sqrt{(1+\frac{\zeta^2}{Z_R^2})}},$$
$$\varphi = \frac{\xi^2+\eta^2}{2\sigma_T^2(\frac{Z_R}{\zeta}+\frac{\zeta}{Z_R})} - \mathrm{artg}\left(\frac{\zeta}{Z_R}\right), \quad (3)$$

where (ξ, η, ζ) are proper coordinates of the laser beam, connected with the laboratory frame ones by $\xi = x$, $\eta = y\cos\alpha - z\sin\alpha$ and $\zeta = y\sin\alpha + z\cos\alpha$ (see Fig. 3). Moreover, E_L is the total energy delivered by the laser, Z_R the Rayleigh length, σ_z the longitudinal and σ_T the transverse rms dimensions of the laser field profiles. In particular, the system is a Ti:sapphire laser ($\lambda_0 = 800$ nm), with $E_L < 7$ J, a temporal rms duration that in the first experiments will be of few ps and a waist diameter $W_0 = 2\sigma_T$ that can be diminished up to 15 μm. The interaction is head to head ($\delta = 0$). Taking $E_L = 1$ J, $W_0 = 25$ μm, $\sigma_z = 4$ ps, and with the beam described in the previous paragraph, X/γ photons with energy of 150 keV can be obtained. Numerical tools [45] based on Eqs. (2) and (3) permit one to quantify the number of photons emitted and the resulting bandwidth.

If the electron beam is formed by two beamlets characterized by two different values of the Lorentz factor γ_l with $l = 1, 2$, the radiation contains two groups of photons whose frequencies are centered around the two nominal resonances:

$$\nu_{p,l} \approx \nu_0 \frac{1 - \underline{e}_k \cdot \underline{\beta}_l}{1 - \underline{n} \cdot \underline{\beta}_l} \approx \frac{4\gamma_l^2\nu_0}{1+\Psi_l^2}, \quad (4)$$

where $\Psi_l = \gamma_l\theta_l$ and θ_l is the angle between each beamlet mean direction and the observer. Both ensembles of frequency values are distributed according to the angle-energy correlation typical of the Thomson/Compton process. Since the Thomson radiation is naturally broadband and its bandwidth is controlled by shrinking the limiting acceptance angle $\theta_{\max}$, two different frequency lines can be resolved if

$$\frac{|\nu_{p,1} - \nu_{p,2}|}{\langle\nu_p\rangle} \gtrsim \left[\frac{\Delta\nu_{p,\bar{l}}}{\nu_{p,\bar{l}}}\right]_{\mathrm{FWHM}}, \quad (5)$$

where $\langle\nu_p\rangle$ is the mean frequency value and the right-hand side is the FWHM relative bandwidth of the largest spectral line, individuated with the index $\bar{l}$. Simple scaling laws, validated by comparison with simulations in the linear regime, show that the relative rms bandwidth $\frac{\Delta\nu_p}{\nu_p}$ scales with the quadratic sum of the rms contributes due respectively to the acceptance $\Psi_{\max} = \gamma\theta_{\max}$, i.e., $[\frac{\Delta\nu_p}{\nu_p}]_\Psi \approx 0.29\Psi_{\max}^2$ (0.29 being the coefficient needed to express the rms value in terms of the limiting acceptance angle), to the normalized emittance ϵ_n in the limit of round electron beam $[\frac{\Delta\nu_p}{\nu_p}]_\epsilon \approx (\frac{\epsilon_n}{\sigma_x})^2$, to the rms energy spread $[\frac{\Delta\nu_p}{\nu_p}]_{\Delta\gamma} \approx \frac{\Delta\gamma}{\gamma}$, to the rms laser natural bandwidth $[\frac{\Delta\nu_p}{\nu_p}]_{\Delta\nu} \approx \frac{\Delta\nu_0}{\nu_0}$, diffraction $[\frac{\Delta\nu_p}{\nu_p}]_d \approx (\frac{M^2\lambda_L}{2\pi W_0})$ and temporal profile $[\frac{\Delta\nu_p}{\nu_p}]_{\sigma_z} \approx \frac{a_0^2/3}{1+a_0^2/2}$. These contributions sum quadratically when the spectrum is almost Gaussian, giving, in this limit, the expression

$$\frac{\Delta\nu_p}{\nu_p} \approx \sqrt{0.09\Psi_{\max}^4 + \left(\frac{\epsilon_n}{\sigma_x}\right)^4 + \left[\frac{\Delta\nu_p}{\nu_p}\right]_{\Delta\gamma}^2 + \left[\frac{\Delta\nu_p}{\nu_p}\right]_L^2}, \quad (6)$$

where the last term gathers all the broadenings due to the laser, that in our case are often negligible. Another cause of spectral broadening is due to nonlinear effects. In our case, however, we consider situations where the laser parameter a_0 is less than or of the order of 0.1, and the nonlinear effects can be neglected. The emittance term $(\frac{\epsilon_n}{\sigma_x})^2$ can be minimized by changing the transverse size of the beam by means of the focusing system. Assuming the emittance at about 1.86 mm mrad as in the case of beam (A), the broadening due to the emittance is negligible at 1 mrad when the transverse size of the electron beam is larger than 20 μm. Once the operation of controlled focusing is performed, the main broadening cause is ascribable to the acceptance, and the two spectral lines of the double color radiation can be distinguished under the following condition:

$$\frac{|\nu_{p,1} - \nu_{p,2}|}{\langle\nu_p\rangle} \gtrsim 0.68\Psi_{\max}^2, \quad (7)$$

the factor 0.68 coming from the relationship between rms and FWHM values. Inserting the parameters relevant to our cases, we obtain two separated lines in correspondence to an acceptance angle less than or about $\theta_{\max} \approx 1.1$ mrad. From a simple model based on the luminosity of the system [45], assuming Gaussian profiles for both laser and electron distributions with similar transverse waists, one can give an estimate of the total number of photons collected in $\theta_{\max}$, which is given by

$$N \approx \frac{2\,10^8 E_L Q\Psi_{\max}^2}{h\nu_L\sigma_x^2} \approx \frac{0.29\,10^9 E_L Q}{h\nu_L\sigma_x^2}\frac{|\nu_{p,1} - \nu_{p,2}|}{\langle\nu_p\rangle} \quad (8)$$

(Q being the electron charge in pC, $h\nu_L$ in eV, the other quantities in MKS), and exceeds 10^6.

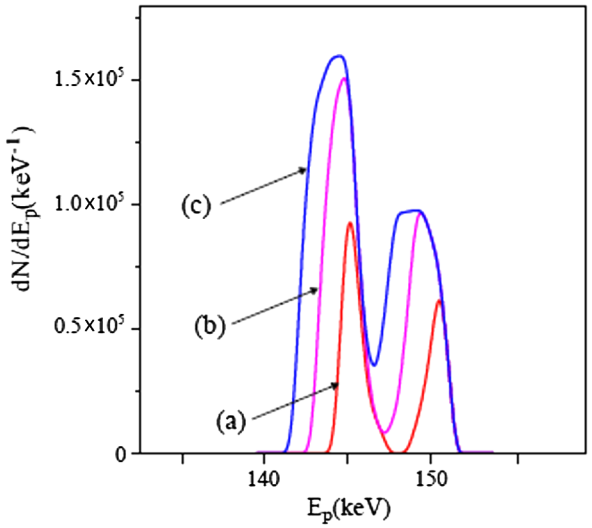

FIG. 4. Spectral density $S = dN/dE_p$ as a function of E_p in the case of beam (A) for different acceptance angles: (a) $\theta_{\max} = 0.5$ mrad, (b) $\theta_{\max} = 0.8$ mrad, and (c) $\theta_{\max} = 1$ mrad.

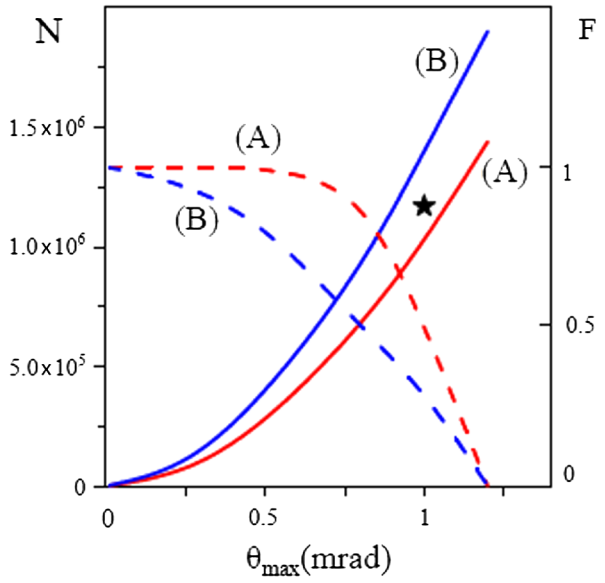

FIG. 6. Number of emitted photons N (solid lines) for beam (A) (red solid line) and (B) (blue solid line) and contrast F (dashed lines) as a function of the acceptance angle $\theta_{\max}$.

Figures 4 and 5 present the spectral density $S = dN/dE_p$, obtained by integrating on the solid angle the double differential spectrum of Eq. (2), converting frequency in energy $E_p = h\nu_p$ and summing over the electrons, as a function of E_p for different acceptance angles and respectively for beams (A) and (B). The numerical results confirm the previous evaluations. Even if beam (B) has a better value of total emittance, the spectrum in Fig. 5 presents a tail on the side of the lower energies that is not present in the other case. This is due to the asymmetry of beam (B) in the transverse phase space. In fact, the beamlet at lower energy has a larger emittance. Figure 6 shows the number of emitted photons as a function of the acceptance angle together with the line contrast $F = [S(\max) - S(\min)]/[S(\max) + S(\min)]$ (min and max being respectively the frequency where the spectral flux is maximum and the minimum value between the two peaks) for the cases analyzed.

The analytical estimates given by Eq. (8) are reported on the figure with a star. The number of photons present in each peak turns out to be sufficiently large to be detected separately with spectroscopic methods or K-edge filters,

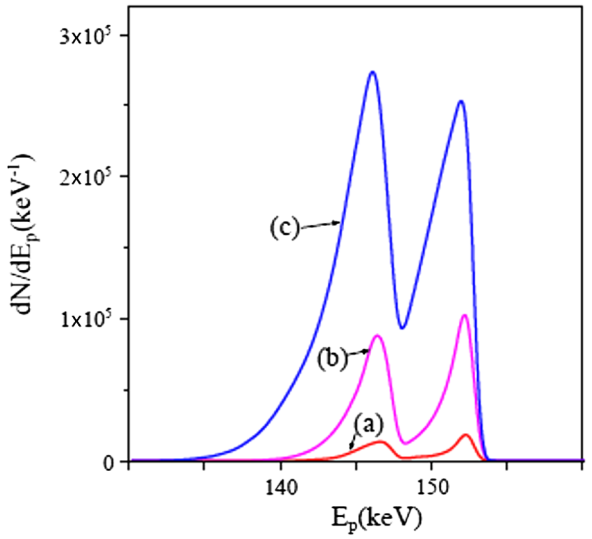

FIG. 5. Spectral density $S = dN/dE_p$ as a function of E_p in the case of beam (B) for different acceptance angles: (a) $\theta_{\max} = 0.2$ mrad, (b) $\theta_{\max} = 0.5$ mrad, and (c) $\theta_{\max} = 1$ mrad.

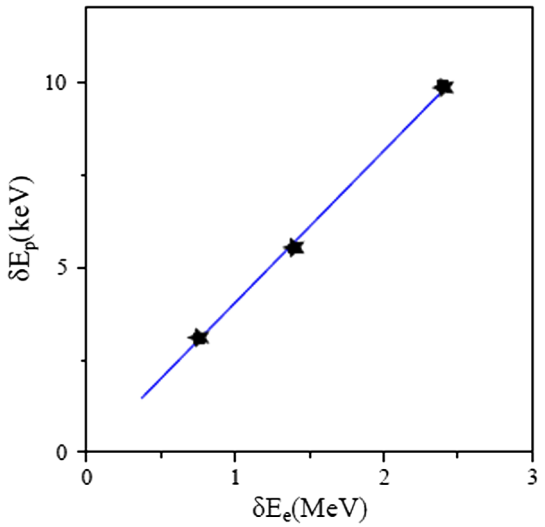

FIG. 7. Photon energy distance $\delta E_p = h|\nu_{p,1} - \nu_{p,2}|$ of the two peaks in keV as a function of the energy gap δE_e between the two electron beamlets in MeV.

depending on the energy of the photons [33]. In Fig. 7, the separation between the spectral lines as a function of the energy separation of the beamlets is shown for bunches similar to beam (A), but obtained with various crystal length and presenting therefore different energy gaps.

The mean frequency of the two-color radiation, instead, can be ruled by changing the rf accelerating gradient in the linac, and extracting the electrons at different energy values. In particular, lowering the electron beam energy down to 50–30 MeV, photon energies ranging from 60 to 20 keV can be produced, exploring therefore regimes of x rays where robust methods for resolving accurately the spectrum exist at SPARC [33].

IV. CONCLUSIONS

In conclusion, we have shown that it is possible to produce two-color x rays with an electron beam with a two level energy distribution. The electron beam has been already studied experimentally at SPARC in the framework of FEL applications. Simulated electron beams, similar to the measured ones, have been used in Thomson/Compton start-to-end numerical calculations, showing to be suitable to produce two-color x rays, interesting for various applications. Acceptance angles of the order of 1 mrad permit one to isolate the spectral lines, achieving a total number of about 10^6 photons with large line contrast. The photon energy can be controlled by changing the extraction condition of the electrons from the linac.

ACKNOWLEDGMENTS

The authors gratefully acknowledge useful and stimulating discussions with the SPARC group, with Professor Pietro Musumeci and Professor Mauro Gambaccini.

[1] C. M. Guenther, B. Pfau, R. Mitzner, B. Siemer, S. Roling, H. Zacharias, O. Kutz, I. Rudolph, D. Schondelmaier, R. Treusch, and S. Eisebitt, Nat. Photonics **5**, 99 (2011).
[2] F. Tavella, N. Stojanovic, G. Geloni, and M. Gensch, Nat. Photonics **5**, 162 (2011).
[3] Y. Ding, F. J. Decker, P. Emma, C. Feng, C. Field, J. Frisch, Z. Huang, J. Krzywinski, H. Loos, J. Welch, J. Wu, and F. Zhou, Phys. Rev. Lett. **109**, 254802 (2012).
[4] P. Finetti, at *The FEL Conference, 2013, TUOBNO02.*
[5] A. H. Zewail, J. Phys. Chem. A **104**, 5660 (2000).
[6] J. F. Cahoon, K. R. Sawyer, J. P. Schlegel, and C. B. Harris, Science **319**, 1820 (2008).
[7] J. D. Biggs, Y. Zhang, D. Healion, and S. Mukamel, J. Chem. Phys. **136**, 174117 (2012).
[8] I. A. Bocharova, A. S. Alnaser, U. Thumm, T. Niederhausen, D. Ray, C. L. Cocke, and I. V. Litvinyuk, Phys. Rev. A **83**, 013417 (2011).
[9] H. Tao, T. K. Allison, T. W. Wright, A. M. Stooke, C. Khurmi, J. van Tilborg, Y. Liu, R. W. Falcone, A. Belkacem, and T. J. Martinez, J. Chem. Phys. **134**, 244306 (2011).
[10] T. K. Allison, H. Tao, W. J. Glover, T. W. Wright *et al.*, J. Chem. Phys. **136**, 124317 (2012).
[11] B. Dierickx, N. Buls, C. Bourgain, C. Breucq, J. Demey, B. Dupont, and A. Defernez, at *The European Optical Society Symposium, Munchen, 2009.*
[12] I. Willekens, B. Dierickx, N. Buls, C. Breucq, A. Schiettecatte, J. de Mey, and C. Bourgain, at *The European Society for Radiography, Vienna, 2011.*
[13] A. A. Lutman, R. Coffee, Y. Ding, Z. Huang, J. Krzywinski, T. Maxwell, M. Messerschmidt, and H.-D. Nuhn, Phys. Rev. Lett. **110**, 134801 (2013).
[14] E. Allaria, F. Bencivenga, R. Borghes, F. Capotondi *et al.*, Nat. Commun. **4**, 2476 (2013).
[15] B. Mahieu, E. Allaria, D. Castronovo, M. B. Danailov *et al.*, Opt. Express **21**, 22728 (2013).
[16] V. Petrillo, M. Anania, M. Artioli, A. Bacci, M. Bellaveglia, E. Chiadroni *et al.*, Phys. Rev. Lett. **111**, 114802 (2013).
[17] A. Marinelli, A. A. Lutman, J. Wu, D. Ratner, S. Gilevich, F. J. Decker, J. Turner, H. Loos, Y. Ding, J. Krzywinski, Y. Feng, H. D. Nuhn, J. Welch, T. Maxwell, C. Behrens, R. Coffee, Z. Huang, and C. Pellegrini, at *The FEL Conference, 2013, WEPSO40.*
[18] H. P. Freund and P. G. O'Shea, Phys. Rev. Lett. **84**, 2861 (2000).
[19] D. Xiang, Z. Huang, and G. Stupakov, Phys. Rev. ST Accel. Beams **12**, 060701 (2009).
[20] A. Zholents and G. Penn, Nucl. Instrum. Methods Phys. Res., Sect. A **612**, 254 (2010).
[21] N. R. Thompson and B. McNeil, Phys. Rev. Lett. **100**, 203901 (2008).
[22] I. V. Pogorelsky, I. Ben-Zvi, T. Hirose, S. Kashiwagi *et al.*, Phys. Rev. ST Accel. Beams **3**, 090702 (2000).
[23] W. Brown, S. Anderson, C. Barty, S. Betts, R. Booth, J. Crane *et al.*, Phys. Rev. ST Accel. Beams **7**, 060702 (2004); F. V. Hartemann, A. M. Tremaine, S. G. Anderson, C. P. J. Barty, S. M. Betts, R. Booth, W. J. Brown, J. K. Crane, R. R. Cross, D. J. Gibson, D. N. Fittinghoff, J. Kuba, G. P. Le Sage, D. R. Slaughter, A. J. Wootton, E. P. Hartouni, P. T. Springer, J. B. Rosenzweig, and A. K. Kerman, Laser Part. Beams **22**, 221 (2004).
[24] M. Babzien *et al.*, Phys. Rev. Lett. **96**, 054802 (2006).
[25] M. Bech, O. Bunk, C. David, R. Ruth, J. Rifkin, R. Loewen, R. Feidenhans'l, and F. Pfeiffer, J. Synchrotron Radiat. **16**, 43 (2009).
[26] D. J. Gibson, F. Albert, S. G. Anderson, S. M. Betts *et al.*, Phys. Rev. ST Accel. Beams **13**, 070703 (2010).
[27] R. Kuroda, H. Toyokawa, M. Yasumoto, H. Ikeura-Sekiguchi, M. Koike, K. Yamada, T. Yanagida, T. Nakajyo, F. Sakai, and K. Mori, Nucl. Instrum. Methods Phys. Res., Sect. A **637**, S183 (2011).
[28] C. Sun and Y. K. Wu, Phys. Rev. ST Accel. Beams **14**, 044701 (2011).
[29] Y. Du, L. Yan, J. Hua, Q. Du, Z. Zhang, R. Li, H. Qian, W. Huang, H. Chen, and C. Tang, Rev. Sci. Instrum. **84**, 053301 (2013).
[30] A. Jochmann, A. Irman, U. Lehnert, J. P. Couperus *et al.*, Nucl. Instrum. Methods Phys. Res., Sect. B **309**, 214 (2013); A. Jochmann, A. Irman, M. Bussmann, J. P. Couperus, T. E. Cowan, A. D. Debus, M. Kuntzsch, K. W. D. Ledingham, U. Lehnert, R. Sauerbrey, H. P. Schlenvoigt,

D. Seipt, Th. Stohlker, D. B. Thorn, S. Trotsenko, A. Wagner, and U. Schramm, Phys. Rev. Lett. **111**, 114803 (2013).

[31] G. Priebe *et al.*, Laser Part. Beams **26**, 649 (2008); D. Laundy, G. Priebe, S. P. Jamison, D. M. Graham, P. J. Phillips, S. L. Smith, Y. Saveliev, S. Vassilev, and E. A. Seddon, Nucl. Instrum. Methods Phys. Res., Sect. A **689**, 108 (2012).

[32] M. Babzien, I. Ben-Zvi, K. Kusche, I. V. Pavlishin, I. V. Pogorelsky, D. P. Siddons, V. Yakimenko, D. Cline, F. Zhou, T. Hirose, Y. Kamiya, T. Kumita, T. Omori, J. Urakawa, and K. Yokoya, Phys. Rev. Lett. **96**, 054802 (2006).

[33] B. Golosio, M. Endrizzi, P. Oliva, P. Delogu, M. Carpinelli, I. Pogorelsky, and V. Yakimenko, Appl. Phys. Lett. **100**, 164104 (2012).

[34] P. Oliva, A. Bacci, U. Bottigli, M. Carpinelli *et al.*, Nucl. Instrum. Methods Phys. Res., Sect. A **615**, 93 (2010).

[35] M. Ferrario, D. Alesini, M. P. Anania, A. Bacci *et al.*, Nucl. Instrum. Methods Phys. Res., Sect. B **309**, 183 (2013).

[36] L. A. Gizzi, A. Bacci, S. Betti *et al.*, Eur. Phys. J. Spec. Top. **175**, 3 (2009).

[37] L. Giannessi *et al.*, Phys. Rev. ST Accel. Beams **14**, 060712 (2011).

[38] M. Boscolo, I. Boscolo, F. Castelli, S. Cialdi, M. Ferrario, V. Petrillo, and C. Vaccarezza, Nucl. Instrum. Methods Phys. Res., Sect. A **593**, 106 (2008).

[39] M. Ferrario *et al.*, Nucl. Instrum. Methods Phys. Res., Sect. A **637**, S43 (2011).

[40] L. Giannessi *et al.*, Phys. Rev. Lett. **106**, 144801 (2011).

[41] G. Marcus *et al.*, Appl. Phys. Lett. **101**, 134102 (2012).

[42] E. Chiadroni *et al.*, Rev. Sci. Instrum. **84**, 022703 (2013).

[43] TSTEP is an upgraded version of PARMELA; see L. M. Young, Los Alamos National Laboratory Report No. LA-UR-96-1835.

[44] K. Floetmann, ASTRA, http://desy.de/mpyo/Astra_dokumentation/.

[45] V. Petrillo, A. Bacci, R. Ben Al Zinati, I. Chaikovska, C. Curatolo, M. Ferrario, C. Maroli, C. Ronsivalle, A. R. Rossi, L. Serafini, P. Tomassini, C. Vaccarezza, and A. Variola, Nucl. Instrum. Methods Phys. Res., Sect. A **693**, 109 (2012).

[46] J. D. Jackson, *Classical Electrodynamics* (Wiley, New York, 1998), 3rd ed.

[47] A. Bacci, M. Ferrario, C. Maroli, V. Petrillo, and L. Serafini, Phys. Rev. ST Accel. Beams **9**, 060704 (2006).

[48] V. Petrillo, L. Serafini, and P. Tomassini, Phys. Rev. ST Accel. Beams **11**, 070703 (2008).

[49] P. Tomassini *et al.*, IEEE Trans. Plasma Sci. **36**, 1782 (2008).

[50] C. Maroli, V. Petrillo, L. Serafini, and P. Tomassini, Phys. Rev. ST Accel. Beams **16**, 030706 (2013).